Chemical Engineering Journal 151 (2009) 262–274

Contents lists available at ScienceDirect

Chemical Engineering Journal

journal homepage: www.elsevier.com/locate/cej

Coupling a mathematical and a fuzzy logic-based model for prediction of zinc ions separation from wastewater using electrodialysis

Mohtada Sadrzadeh, Ali Ghadimi, Toraj Mohammadi*

Research Centre for Membrane Separation Processes, Faculty of Chemical Engineering, Iran University of Science and Technology (IUST), Narmak, Tehran, Iran

ARTICLE INFO

Article history:
Received 4 January 2009
Received in revised form 21 February 2009
Accepted 1 March 2009

Keywords:
Fuzzy logic
Electrodialysis
Mathematical modeling
Coupled model
Zinc ions separation

ABSTRACT

This paper presents experimental data, a fuzzy logic (FL) model, a mathematical model (MM) and a coupled MM–FL model for a laboratory scale electrodialysis (ED) cell. The aim was to predict separation percent (SP) of zinc ions as a function of concentration, temperature, flow rate and voltage. At first, a Sugeno type FL inference system was applied to model zinc ions separation from wastewater using ED. FL modeling results showed that there is an excellent agreement between the experimental data and the predicted values, with mean squared relative error (MSRE) of less than 0.01. Then, the results of a previously developed MM were presented. The MM related SP to hydrodynamic dimension of the ED cell and operation conditions via two distinct parameters. This ability favored the MM for scale-up applications. However, based on MSRE of the MM (about 24), it could not obviously predict the experimental data as well as FL. Hence, as a final step, the MM was coupled with FL to achieve benefits of both. It was found out that the developed coupled model (MM–FL) is able to predict SP of zinc ions at all operating condition and almost every dimension to a high degree of accuracy (MSRE = 0.05).

1. Introduction

Electrodialysis (ED) is an electro-membrane process for separation of ions across charged membranes from one solution to another with the aid of an electrical potential difference used as a driving force. This process has been widely used for production of drinking and process water from brackish water and sea water, treatment of industrial effluents, recovery of useful materials from effluents and salt production. The basic principles and applications of ED were reviewed in the literature [1–6].

In order to improve the performance of ED process, optimization (operating and design) and analysis of the process should be accomplished. Modeling and simulation are tools to achieve these objectives. However, modeling of a process covers a broad spectrum. At one extreme lie theoretical (or parametric) models based on fundamental knowledge of the process. These models are also called knowledge-based models. At the other end lie empirical (or non-parametric) models which do not rely on the fundamental principles which governing the process [7–9].

A large majority of modeling works on ED process are theoretical which are developed using Nernst–Planck equation for diffusions, convection and migration of charged species in electric field and a material balance equation such as Maxwell–Stefan equation [10–28]. The Maxwell–Stefan equation represents the simplest mathematical tool for linking the flux of a generic species through the membrane with its interfacial concentrations at the membrane left- and right-sides, as well as with the external electrical voltage applied to the ED electrodes [29]. To overcome the main problem in application of the Maxwell–Stefan mass transfer model to ED process, i.e. the large number of species diffusivities in the bulk solution and the membrane phase [30], the Nernst–Planck relationship is largely used to describe diffusion and electro-migration contributions to ion transport in ion exchange membranes.

Most of these models are obviously derived from physical descriptions and understanding of the ED process under the assumption of Donnan equilibrium. Basic electrochemistry rules such as Kohlrausch law, Nernst–Einstein equation, Einstein equation, and Debye–Huckel–Onsager theory are also used everywhere needed [20,24].

Most theoretical models can be used for different scale of ED cells and ions. These types of models are very useful for scale-up applications. However, as mentioned above, they are mathematically complex, computationally expensive and they ideally require a very detailed knowledge of the ED process as well as characterization of the membranes. Therefore, there is a need to find an alternative means for predicting process performance by exploiting available process data and extending them to unavailable data. Fuzzy logic (FL) inference systems and artificial neural networks are capable of modeling highly complex and non-linear processes such as ED. The main limitation of these types of modeling is that,

* Corresponding author. Tel.: +98 21 77240496; fax: +98 21 77240495.
E-mail address: torajmohammadi@iust.ac.ir (T. Mohammadi).

1385-8947/$ – see front matter © 2009 Elsevier B.V. All rights reserved.
doi:10.1016/j.cej.2009.03.003

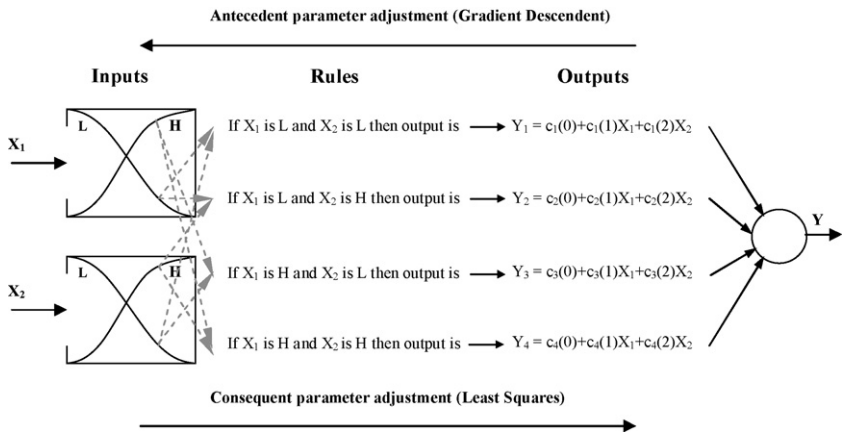

Fig. 1. ANFIS architecture of the input–output system.

they only can be utilized for a specific experiment. In spite of their outstanding ability in predicting the behavior of processes, they are not as flexible as theoretical models to be employed for scale-up.

Artificial neural network has been used in a wide range of membrane process applications (reverse osmosis, nanofiltration, ultrafiltration, microfiltration, membrane filtration, gas separation, membrane bioreactor and fuel cell) [31]. Recently, ED process was modeled using a multilayer perceptron neural network with two hidden layers [31]. Fuzzy control system was limitedly applied in membrane processes [32–36]. However, there are a few records in the literature which applied FL for prediction of membrane processes behaviors [37–39].

In this study, a FL inference system was initially used to model an ED process. The FL model was successful to predict separation percent (SP) of zinc ions in the limit of experimented levels of operating parameters using a laboratory scale ED cell, excellently. Then, the results of a previously developed mathematical model (MM) were presented [20,24]. The main advantage of MM was to relate SP to hydrodynamic dimension of the ED cell and operation conditions via two distinct parameters. However, the MM could not predict the experimental data as well as FL. Finally, the MM was coupled with FL to overcome the above mentioned shortcomings of both models. The developed coupled model (MM–FL) was realized to be able to predict SP of zinc ions at all operating conditions and almost every dimension to a high degree of accuracy.

2. FL theory

FL was developed by Zadeh in 1965. Basically, FL is a multivalued logic that allows intermediate values to be defined between conventional evaluations like true/false, yes/no, high/low, etc. Notions like rather tall or very fast can be formulated mathematically and processed by computers, in order to apply a more human-like way of thinking in the programming of computers.

The use of fuzzy set theory allows the user to include the unavoidable imprecision in the data. Fuzzy inference is the actual process of mapping from a given set of input variables to an output based on a set of fuzzy rules. The essence of the modeling is to identify fuzzy rules. Four fundamental units are necessary for the successful application of any fuzzy modeling approach. These are, namely, the fuzzification unit, the knowledge base (which is composed of the database and the rule base), the inference engine unit and the defuzzification unit.

In the fuzzification unit, the input and output variables are fuzzified by considering convenient linguistic subsets such as high, medium, low, heavy, light, hot, warm, big, small, etc. Partition of variable into groups is not a very easy task. Various methods have been developed in the literature, such as the neural network-based method [40], the inductive learning [41], the genetic algorithm [42], the fuzzy clustering [43] and uses of statistics [44].

In knowledge base unit, fuzzy IF–THEN rules are constructed based on the expert knowledge and/or on the basis of available data. The rules provide a transition between input and output fuzzy sets. Premise part input fuzzy membership functions (MFs) are combined interchangeably with a logical “and” or “or” a conjunction whereas the rules are combined with the logical “or” the conjunction.

In the inference engine unit, the implication part of a fuzzy system is defined as the forming of the consequent MFs based on the membership degrees of the premise (antecedent) part.

In the defuzzification unit, the result appears as a fuzzy set is defuzzified to calculate a crisp value, which is asked for engineering applications.

In the applications of the fuzzy system in control and forecasting, there are mainly two approaches, namely, Mamdani and Sugeno methods [45]. For the first approach, there are clear procedures i.e. fuzzification, inference and defuzzificiation procedures. The main difference between Mamdani and Sugeno approaches is originated from defuzzification procedure. In the Mamdani approach, each IF–THEN rule produces a fuzzy set for the output variable, and hence the step of defuzzification is indispensable so as to obtain crisp values of the output variable. However, in Sugeno method, outcome of each IF–THEN inference rule is a scalar rather than a fuzzy set for the output variable. Defuzzification procedure is completed simply in Sugeno method by taking the weighted average of the rule outcome.

The main problem with the Sugeno FL modeling is related to the choice of the modeling parameters. For this reason, the adaptive network-based fuzzy inference system (ANFIS) methodology is applied to estimate the parameters of the membership and the consequent functions [46]. ANFIS is a certain type of the FL models. In this approach, outputs of the knowledge base unit are crisp values and do not need defuzzification. The general scheme of the ANFIS is shown in Fig. 1. Fig. 2 depicts the two-dimensional input space where X_1 and X_2 are partitioned into four symmetric triangular fuzzy sets. The Sugeno approach has fuzzy sets in the premise part only and IF–THEN control rules are given as follows:

$$R_r: \quad \text{IF } X_1 \text{ is } S_r^{(1)}, X_2 \text{ is } S_r^{(2)}, \ldots, X_p \text{ is } S_r^{(n)} \quad \text{THEN } Y_r = f_r(X_1, X_2, \ldots, X_n) \tag{1}$$

where $S_r^{(i)}$ is a fuzzy set corresponding to a partitioned domain of the input variable X_j in the rth IF–THEN rule, n is the number of input variables, f_r is a function of the n input variables, and finally Y_r is the output of the rth IF–THEN inference rule R_r.

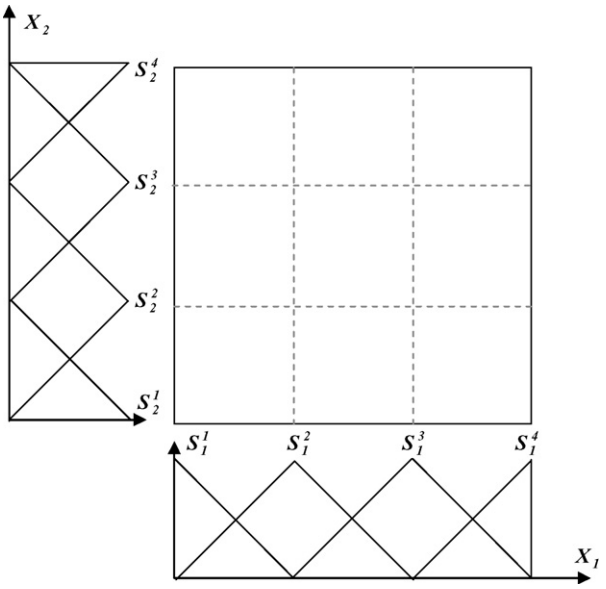

Fig. 2. Fuzzy partition in the two-dimensional space.

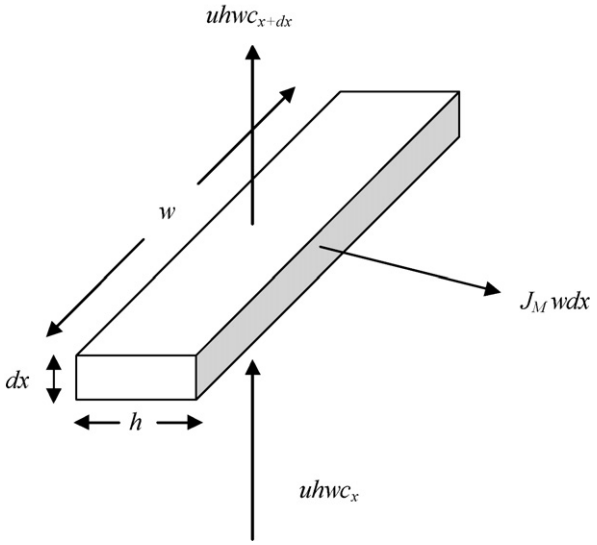

Fig. 3. Differential element of the dilute compartment.

The general algorithm of the Sugeno inference system is expressed as follows [45]. It is assumed that there are R_r ($r = 1, 2, 3, \ldots, k$) rules in the above mentioned form.

1. For each implication R_i, Y_i is calculated by the function f_i in the consequence part:

$$Y_i = f_i(X_1, X_2, \ldots, X_n) = c_r(0) + c_r(1)X_1 + c_r(2)X_2 + \cdots + c_r(n)X_n \tag{2}$$

2. The weights are calculated as follows:

$$r_r = (m_1^r \wedge m_2^r \wedge \cdots \wedge m_n^r)P^r \tag{3}$$

where $m_1^r, m_2^r, \ldots, m_k^r$ denote the α cuts of MFs according to input values for the rth rule. An α cut of a fuzzy set A (A_α) is a crisp set, which contains all the elements in U that have membership values greater than or equal to α ($x \in U \mid \mathrm{MF} \geq \alpha$) in A. The universe of discourse U is the n-dimensional Euclidean space R^n. The occurrence probability is shown by P^r and $\wedge$ stands for min or production operation. For the sake of simplicity P^r is taken as equal to 1.The final output Y inferred from k implications is given as the weighted average of all Y_r with the weights r_r as

$$Y = \frac{\sum_{r=1}^{n} r_r Y_r}{\sum_{r=1}^{n} r_r} \tag{4}$$

3. Mathematical modeling

A differential element of the dilute compartment is illustrated in Fig. 3. The steady state mass balance of lead ions in the compartment is as follows:

$$uhwC_x - uhwC_{x+dx} = J_M w\ dx \tag{5}$$

Also, the molar flux through the dilute compartment in term of current density is as follows:

$$J_M = \eta \frac{i}{F} = \frac{\eta}{F}\frac{dI}{dA_m} \tag{6}$$

where $A_m = lw$, l, h and w are the channel dimensions, η is the current efficiency, F is the Faraday constant and i is the current density. Assuming constant concentration in the cell compartment ($dI/dAm = I/Am$), the following differential equation is obtained [47]:

$$uh\,dC = -\frac{I}{A_m}\frac{\eta}{F}dx \tag{7}$$

In order to be able to use integrate form of this equation with operational variables, η needs to be verified. At any point, molar flux can be written as follows:

$$J_M = k(C_{bulk} - C_i) = k\ \Delta C \tag{8}$$

where C_{bulk} and C_i are concentrations at the bulk of dilute stream and at the membrane surface, respectively. Due to very small distance between two membranes, ΔC can be assumed to be constant

Table 1
Electrochemistry rules to find the functionality of electrolyte resistance (R).

(1) Electrolyte resistance	$R = \frac{h}{\kappa A}$	(2) Electrolyte conductivity	$\kappa = \Lambda_M C$
(3) Molar conductivity	$\Lambda_M = \Lambda_M^\circ - KC^{0.5}$	(4) Limiting molar conductivity[a]	$\Lambda_M^\circ = \nu_+\lambda_+ + \nu_-\lambda_-$
(5) Ion molar conductivity	$\lambda_\pm = \frac{z_\pm F D_\pm}{\Re T}$	(6) Diffusion coefficient	$D_\pm = \frac{\upsilon_\pm \Re T}{z_\pm F}$
(7) Ion mobility[b]	$\upsilon_\pm = \frac{z_\pm e}{6\pi\mu a_\pm}$	(8) Kohlrausch coefficient	$K = \zeta + \psi\Lambda_m^\circ$
(9) Debye–Huckel–Onsager coefficient	$\zeta = \frac{z^2 eF^2}{3\pi\mu}\left(\frac{2}{\varepsilon\Re T}\right)^{0.5}$	(10) Debye–Huckel–Onsager coefficient	$\psi = \frac{qz^3 eF^2}{24\pi\varepsilon\Re T}\left(\frac{2}{\varepsilon\Re T}\right)^{0.5}$
(11) Electric permittivity[c]	$\varepsilon = \varepsilon_r\varepsilon_0$	(12) Relative permittivity	$\varepsilon_r = 185.765 - 0.35963T$
(13) Constant[d]	$q = \frac{2\omega z_+ z_-(\lambda_+ + \lambda_-)}{(z_+ + z_-)(z_+\lambda_- + z_-\lambda_+)}$	(14) Constant[e]	$\omega = \frac{z_+ z_-(\lambda_+ + \lambda_-)}{(z_+ + z_-)(z_+\lambda_+ + z_-\lambda_-)}$

[a] Molar conductivity in the limit of zero concentration of an electrolyte. ν_+ and ν_- are the numbers of cations and anions per an electrolyte molecule (e.g. $\nu_+ = \nu_- = 1$ for $PbSO_4$). z_+ and z_- are cation and anion valances. For n–n electrolytes such as $PbSO_4$ $z_+ = z_- = z$.

[b] a in this equation is the ion diameter.

[c] ε_0 is the vacuum permittivity ($8.854 \times 10^{-12}\ C^2\ J^{-1}\ m^{-1}$).

[d] For 1–1, 2–2 and n–n electrolytes $\omega = 0.5$.

[e] $q = 0.586$ and 2.343 for 1–1 electrolyte and 2–2 electrolyte, respectively.

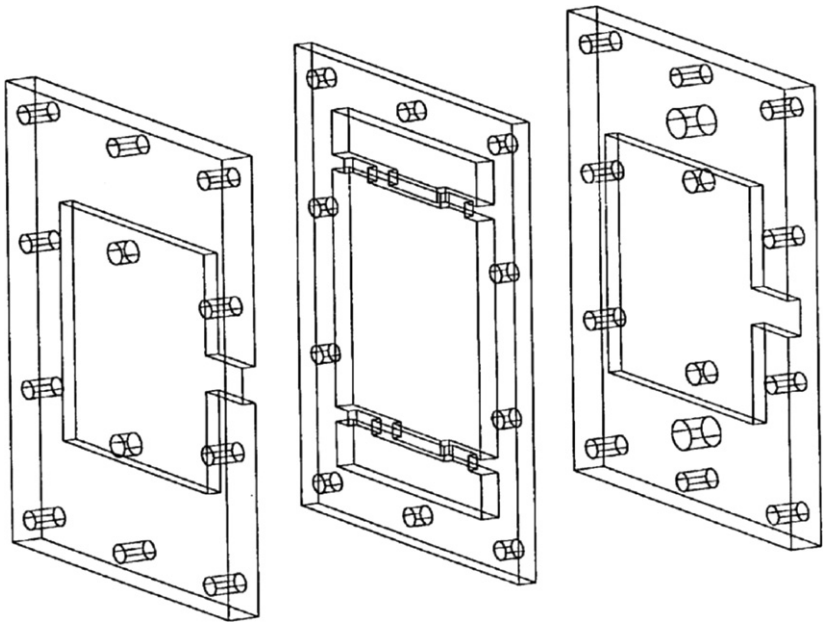

Fig. 4. Laboratory scale plate and frame ED cell.

along the membrane surface [47]. Hence, Eqs. (6) and (8) can be combined as follows:

$$\eta = \frac{\Delta CFA_m}{I} k = \gamma' k \tag{9}$$

According to the literature, k is calculated as follows [48]:

$$k = 3.30 D^{2/3} \left(\frac{Q_d}{hA_d l} \right)^{1/3} \tag{10}$$

In ED, the basic relations between current (I), effective electrical motive force (E) and system resistance (R) can be described by Ohm's law:

$$I = \frac{E}{NR} \tag{11}$$

where N is the number of cells which is 1 in this study. Neglecting membranes resistances, solution resistance can be expressed as a function of concentration and temperature ($f(c,T)$) [3,20,49]. Table 1 shows how electrochemistry rules were applied sequentially to find this functionality [20]. Using equations in this table, the following equation can be derived:

$$R = \frac{h}{CA(x' - y'C^{0.5} - x'z'C^{0.5})} \tag{12}$$

where

$$x' = \frac{eFz^2}{6\pi\mu} \left(\frac{1}{a_+} + \frac{1}{a_-} \right), \quad y' = \frac{3.30}{\mu(\varepsilon_r T)^{0.5}} \quad \text{and} \quad z' = \frac{3281587}{(\varepsilon_r T)^{1.5}}.$$

Combination of Eqs. (7)–(12) and integrating both sides using the following boundary condition result in an expression for the model parameter (γ):

At $x = 0 \quad C = C_0$

$$\gamma = -\frac{Q_d^{2/3}}{ET^{2/3}} \frac{h^{5/3}}{(lw)^{2/3}} \left(\frac{6\pi a}{e\Re} \right)^{2/3} (F\mu)^{5/3} \int_{C_0}^{C} f(C,T)\, dC \tag{13}$$

Using a simple change of variable, Eq. (13) can be written as a function of SP.

$$\gamma = \varphi \times \beta \tag{14}$$

where

$$\varphi = -\frac{Q_d^{2/3} \mu^{5/3}}{C_0 E T^{2/3}} \mathrm{Ln} \left[\frac{(\delta + \sigma)\sqrt{1 - \mathrm{SP}}}{\delta + \sigma\sqrt{1 - \mathrm{SP}}} \right] \tag{15}$$

and

$$\beta = 75 \frac{h^{5/3}}{(lw)^{2/3}} \left(\frac{6\pi a}{e\Re} \right)^{2/3} F^{5/3} \tag{16}$$

MM is related to operating conditions and ED cell dimension by φ and β parameters, respectively. In Eq. (15), $\theta = -\sqrt{C_0/T}(0.38 + 125/T)$ and $\delta = 0.026$. SP is also defined as

$$\mathrm{SP} = \frac{C_0 - C}{C_0} \times 100 \tag{17}$$

where C_0 and C are the feed and dilute concentrations, respectively. The following equation was fitted for φ as a function of operating parameters using experimental data:

$$\varphi = \frac{1}{(-1.5 \times 10^6/E + 1.15 \times 10^7 C_0^{155/T}/E^{0.001} + 3 \times 10^{17} Q_d^{2.5})} \tag{18}$$

With the aid of Eqs. (14)–(18) and using MATLAB programming software, the model gives SP for various operating conditions as well as different ED cell dimensions. Detailed description of the developed model was presented elsewhere [20,24].

4. Materials and methods

4.1. Materials

An analytical grade salt (99.9% zinc sulfate supplied by Merck) and deionized water were used in all experiments to produce solutions with wastewater qualities. The purpose of these experiments was to study the effect of temperature, voltage, flow rate and feed concentration on the ED cell performance.

4.2. Cell and membranes

A plate and frame ED cell made from Plexiglass (polymethyl methacrylate) was used to conduct the experiments (Fig. 4). The ED cell consisted of three detachable parts and packed with a pair

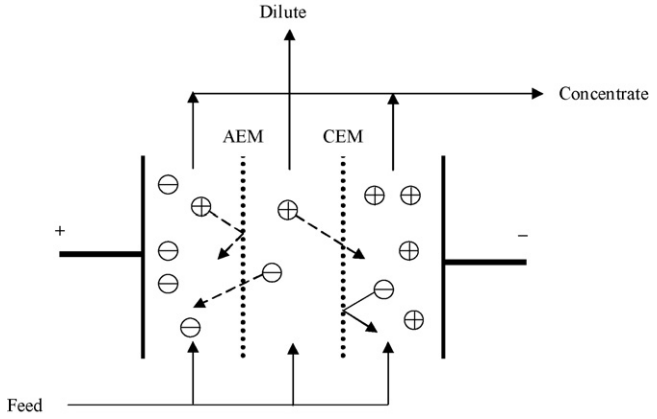

Fig. 5. Schematic view of ED cell.

of cation and anion exchange membranes (CEM and AEM) and a pair of platinum electrodes (anode and cathode). The overall dimensions of length, height and width of the cell were 0.13, 0.06 and 0.09 m, respectively. The membranes had effective area of $0.060 \times 0.065\ m^2$. Rubber O-rings were used to provide a pressure-tight seal between the membrane and the module. Both electrodes were made of pure platinum. The surface area of each electrode was $0.042 \times 0.042\ m^2$. The thickness of dilution cell (center) and each concentrate cell (left and right) were 0.004 and 0.003 m, respectively. Hence, volumes of dilute and concentrate compartments were approximately 15.6×10^{-6} and $11.7 \times 10^{-6}\ m^3$.

Schematic view of the applied ED cell is presented in Fig. 4. Zinc sulfate solution is introduced into the three compartments. CEM allows only cations to permeate, and AEM allows only anions to permeate. These exchange membranes are immersed in wastewater in parallel, as shown in Fig. 5, and an electric current is passed through the solution. The cations migrate to the cathode, and the anions migrate to the anode. Therefore, the solution passing between the membranes is divided into two streams. One is pure water (dilute), and the other is concentrated solution of ions (concentrate). Since ED uses energy at a rate directly proportional to the quantity of ions to be removed, this process is more useful in deionizing wastewater.

Electrical potential is the driving force for transport of ions in ED. This potential is applied from an external power supply through electrodes situated on either end of the ED cell. Current flow in the circuit external to the stack is electronic, i.e., electrons flow through metallic conductors. However, current flow within the stack is electrolytic, i.e., ions flow through solutions. The transfer of electrical charge from electronic to electrolytic conduction is accomplished via electrode reactions [50]:

Table 2
Physical and chemical characteristics of the employed membranes.

Property	Membrane	
	AR204SXR412	CR67, MK111
Reinforcing fabric	Acrylic	Acrylic
Specific weight (mg/cm^2)	13.7	13.7
Thickness (mm)	0.5	0.56–0.58
Burst strength (kg/cm^2)	7.0	7.0
Water content	46% of wet resin only	46% of wet resin only
IEC (meq/dry gram membrane)	2.8	2.4
Chemical stability, pH	1–10	1–10

Anode reaction

$$H_2O \rightarrow 1/2\,O_2(g) + 2H^+ + 2e^-$$

Cathode reaction

$$2H_2O + 2e^- \rightarrow H_2(g) + 2OH^-$$

O_2 and H_2 gas bubbles produced by the anode and cathode reactions can blanket the electrodes and increase the resistance of the ED cell [51]. Hence concentrate streams were disposed off to prevent accumulation of these gases. High values of pH at cathode can cause precipitation of any pH sensitive materials (Zn^{2+} in this study reacts with hydroxide ions and produces $Zn(OH)_2$ precipitate) on CEM, which can raise resistance and even make the ED cell inoperative [51]. At lower flow rates, precipitation is more important. The precipitate was removed by cleaning in place (CIP) using distilled water after each run [5].

AR204SXR412 and CR67, MK111 anion and cation exchange membranes (supplied by Arak petrochemical complex and made by Ionics incorporated) were used in all the experiments. Physical and chemical properties of the applied membranes are presented in Table 2.

4.3. ED setup

ED setup consisted of a feed tank (TK-01) for storing wastewater, two pumps (P-01 and P-02, RESUN submersible pump,

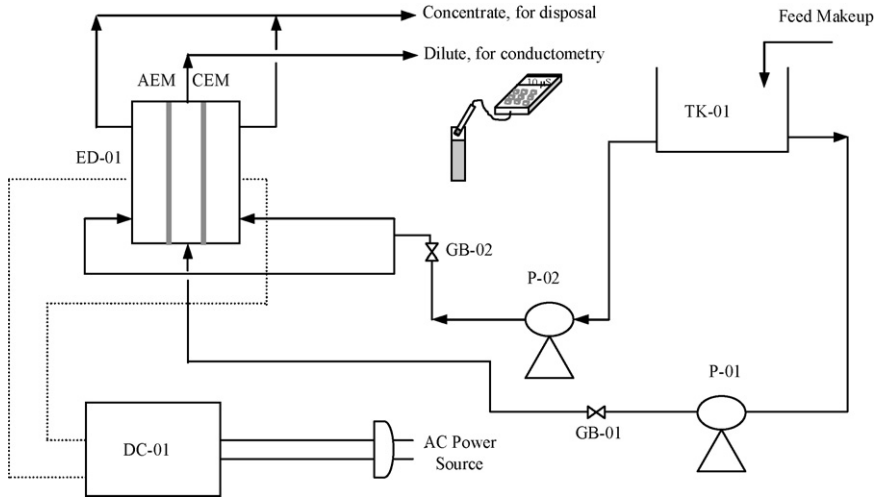

Fig. 6. Schematic view of ED setup.

P = 4 W, total head = 0.5 m), a rectifier (DC-01, RST Spastell TRFO) and two globe valves (GB-01 and GB-02, CHUYU model J11W-200LB) to control the flow rate of feed solution passing through the three compartments of the self-designed ED cell. A simplified diagram of the setup is shown in Fig. 6. As can be observed, the feed solution was passed through the dilute and concentrate compartments, based on once through operation. No cyclic regime was used. Concentrated streams were disposed of and diluted stream was collected for conductometric analysis.

4.4. Experimental design

Experiments were conducted under the limiting current density. Effects of feed concentration (100–1000 ppm), flow rate (0.07×10^{-6}–1.2×10^{-6} m^3/s), temperature (298.15–333.15 K) and voltage (10–30 V) on the performance of ED cell are investigated.

Each experiment lasted for about 15 min to reach steady state condition. After that three samples were taken every 5 min and the average value was reported. Each experiment was repeated three times and the results were presented in average with the maximum deviation of 5%.

It should be noted that there were some factors in the present work which were either uncontrollable or were too expensive to control, such as pH variation, variation of environmental operating conditions, occurring electrolysis on both electrodes, variation of voltage, concentration polarization, etc. These factors are called noise factors. Noise factors may have a negative impact on system performance or may not.

According to the literature, pH effect on the performance of an ED cell is negligible, especially at voltages greater than 10 V [49,52]. Deviation of pH was much more observed in the concentrate compartment (adjacent to electrodes). Since the concentrate stream was disposed of (Fig. 6), it did not affect the dilute stream characteristics. Hence, the variation of pH through the separation process was not monitored.

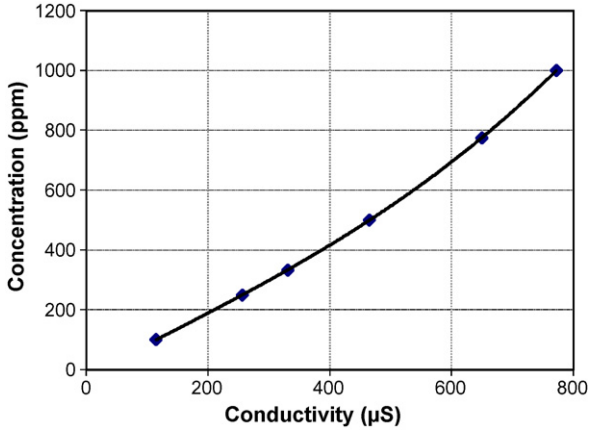

Fig. 7. Calibration curve of the conductometer.

4.5. Analytical method

In all the experiments, a conductometer (HANNA, model HI 8633) was used to measure the amount of ions in the dilute aqueous solution. The conductometer was initially calibrated using zinc sulfate solutions of definite concentrations. Calibration curve of the conductometer is shown in Fig. 7. Then, zinc sulfate concentration in the dilute compartment was measured. Finally, SP was calculated using Eq. (17).

5. Results and discussion

5.1. FL model

A sophisticated intelligent model, based on the Sugeno fuzzy modeling principles, was used to predict the SP of an ED cell. Data spaces were partitioned into fuzzy sets by means of the grid parti-

Table 3
Experimental data used for training and testing the fuzzy model.

Operating parameters					SP (%)	Operating parameters					SP (%)	Operating parameters					SP (%)
T (°C)	C (ppm)	V (V)	I (mA)	Q (mL/s)		T (°C)	C (ppm)	V (V)	I (mA)	Q (mL/s)		T (°C)	C (ppm)	V (V)	I (mA)	Q (mL/s)	
298.15	100	10	0.12	0.07	27.53	313.15	100	10	0.15	0.07	47.66	333.15	100	10	0.20	0.07	53.74
298.15	100	20	0.22	0.07	47.58	313.15	100	20	0.27	0.07	67.71	333.15	100	20	0.36	0.07	73.79
298.15	100	30	0.32	0.07	54.08	313.15	100	30	0.38	0.07	74.21	333.15	100	30	0.51	0.07	80.29
298.15	100	10	0.14	0.70	0.262	313.15	100	10	0.20	0.70	0.884	333.15	100	10	0.27	0.70	2.567
298.15	100	20	0.28	0.70	1.012	313.15	100	20	0.37	0.70	13.71	333.15	100	20	0.50	0.70	19.79
298.15	100	30	0.43	0.70	1.393	313.15	100	30	0.54	0.70	20.21	333.15	100	30	0.72	0.70	26.29
298.15	100	10	0.14	1.20	0.252	313.15	100	10	0.20	1.20	0.683	333.15	100	10	0.27	1.20	1.387
298.15	100	20	0.28	1.20	0.757	313.15	100	20	0.38	1.20	9.420	333.15	100	20	0.51	1.20	15.50
298.15	100	30	0.43	1.20	0.951	313.15	100	30	0.55	1.20	15.92	333.15	100	30	0.74	1.20	22.08
298.15	500	10	0.49	0.07	45.97	313.15	500	10	0.60	0.07	66.10	333.15	500	10	0.80	0.07	72.18
298.15	500	20	0.88	0.07	66.02	313.15	500	20	1.04	0.07	86.15	333.15	500	20	1.37	0.07	92.23
298.15	500	30	1.26	0.07	72.52	313.15	500	30	1.48	0.07	92.65	333.15	500	30	1.95	0.07	98.73
298.15	500	10	0.62	0.70	1.028	313.15	500	10	0.81	0.70	12.10	333.15	500	10	1.09	0.70	18.18
298.15	500	20	1.18	0.70	12.02	313.15	500	20	1.47	0.70	32.15	333.15	500	20	1.97	0.70	38.23
298.15	500	30	1.72	0.70	18.52	313.15	500	30	2.13	0.70	38.65	333.15	500	30	2.85	0.70	44.73
298.15	500	10	0.62	1.20	0.766	313.15	500	10	0.83	1.20	7.810	333.15	500	10	1.11	1.20	13.89
298.15	500	20	1.21	1.20	7.730	313.15	500	20	1.50	1.20	27.86	333.15	500	20	2.01	1.20	33.94
298.15	500	30	1.76	1.20	14.23	313.15	500	30	2.18	1.20	34.36	333.15	500	30	2.92	1.20	40.44
298.15	1000	10	0.90	0.07	44.44	313.15	1000	10	1.10	0.07	64.57	333.15	1000	10	1.46	0.07	70.65
298.15	1000	20	1.61	0.07	64.49	313.15	1000	20	1.93	0.07	84.62	333.15	1000	20	2.55	0.07	90.70
298.15	1000	30	2.32	0.07	70.99	313.15	1000	30	2.75	0.07	91.12	333.15	1000	30	3.63	0.07	97.2
298.15	1000	10	1.09	0.70	1.457	313.15	1000	10	1.44	0.70	10.57	333.15	1000	10	1.94	0.70	16.65
298.15	1000	20	2.11	0.70	10.49	313.15	1000	20	2.64	0.70	30.62	333.15	1000	20	3.54	0.70	36.70
298.15	1000	30	3.09	0.70	16.99	313.15	1000	30	3.84	0.70	37.12	333.15	1000	30	5.14	0.70	43.21
298.15	1000	10	1.09	1.20	0.981	313.15	1000	10	1.47	1.20	6.280	333.15	1000	10	1.97	1.20	12.36
298.15	1000	20	2.15	1.20	6.200	313.15	1000	20	2.70	1.20	26.33	333.15	1000	20	3.61	1.20	32.41
298.15	1000	30	3.14	1.20	12.70	313.15	1000	30	3.92	1.20	32.83	333.15	1000	30	5.21	1.20	40.44

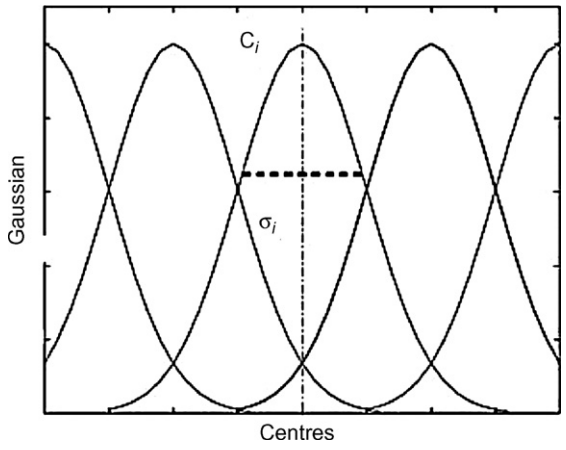

Fig. 8. Gaussian membership function.

tioning method. Training and testing was accomplished with the aid of MATLAB software (version 7.1). ANFIS methodology whit hybrid learning method was applied to estimate the parameters of the applied two-parametric Gaussian membership function (Fig. 8) and the consequent functions. The symmetric Gaussian function depends on two parameters, c and σ, as given by

$$\mu_A(x) = e^{\frac{-(x-c)^2}{2\sigma^2}} \quad (19)$$

where c and σ are the centre and width of the fuzzy set A, respectively.

5.1.1. Input variables selection

Many parameters affect performance of the ED cell:

- ion content of the raw water
- applied electrical potential (current density)
- residence time of solution in the cell compartments (flow rate)
- geometry of cell compartments
- operating temperature
- membrane properties
- feed concentration [6]

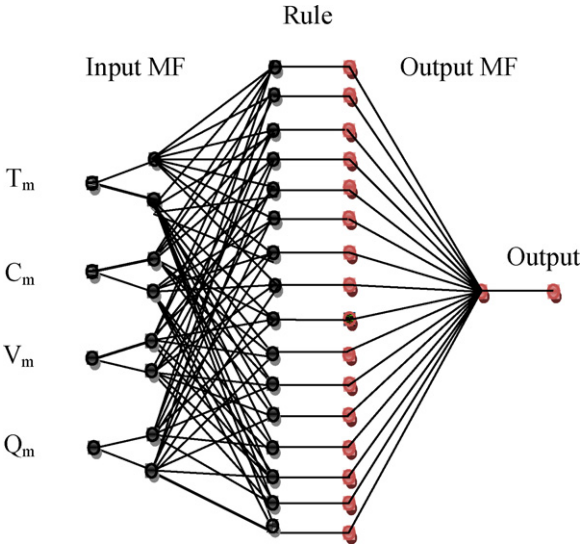

Fig. 9. The ANFIS model structure used in training and testing: 4 input variables, 2 Gaussian membership functions for each variable and 16 rules.

Table 4
Statistical criteria for evaluation of the fuzzy model.

Criterion	Training data	Testing data	Total fuzzy model
MSE	0.1799	0.8503	0.2712
RMSE	0.4242	0.9221	0.5208
R	0.9999	0.9999	0.9998
R^2	0.9998	0.9999	0.9997
MSRE	0.0084	0.0011	0.0074

A technique for laying out the experiments when multiple factors are involved is the factorial design of experiments. This method helps researchers to determine the possible combinations of factors and to identify the best combination. Since it is extremely costly to run a number of experiments to test all combinations, application of the full factorial design of experiments is restricted when many factors and levels are studied.

Hence, according to our previous studies [4–6,47,48], four factors, from the above mentioned parameters, were selected. It is believed that they have the greatest effect on the SP: feed concentration, dilute solution flow rate, voltage and feed inlet temperature.

5.1.2. Training and testing the ANFIS

81 experiments were conducted based on the full factorial design. The results are presented in Table 3. As observed the four factors each at three levels were investigated:

- Temperature (T): 25, 40 and 60 °C
- Concentration (C): 100, 500 and 1000 ppm
- Flow rate (Q): 0.07, 0.7 and 1.2 mL/s
- Voltage (V): 10, 20 and 30 V

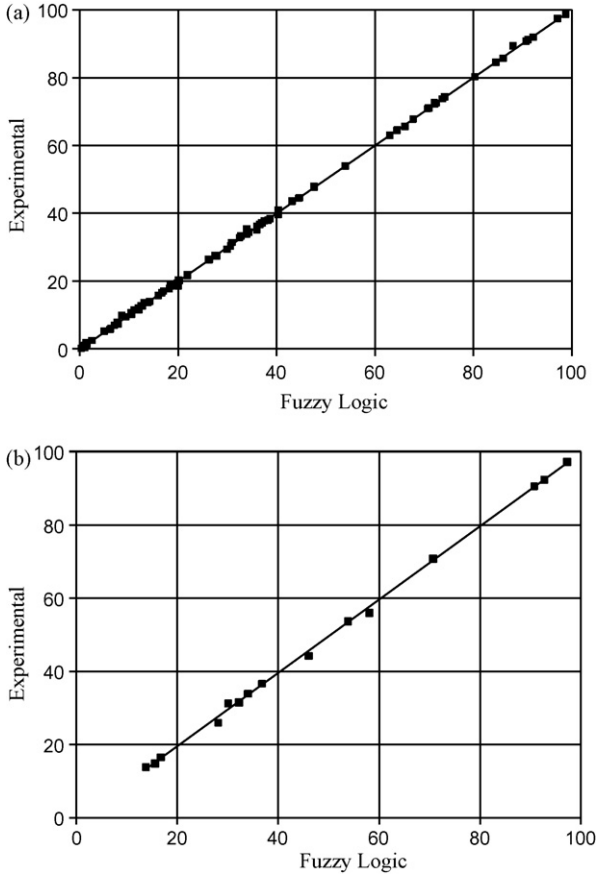

Fig. 10. Performance of FL model in predicting SP: (a) training data, (b) testing data.

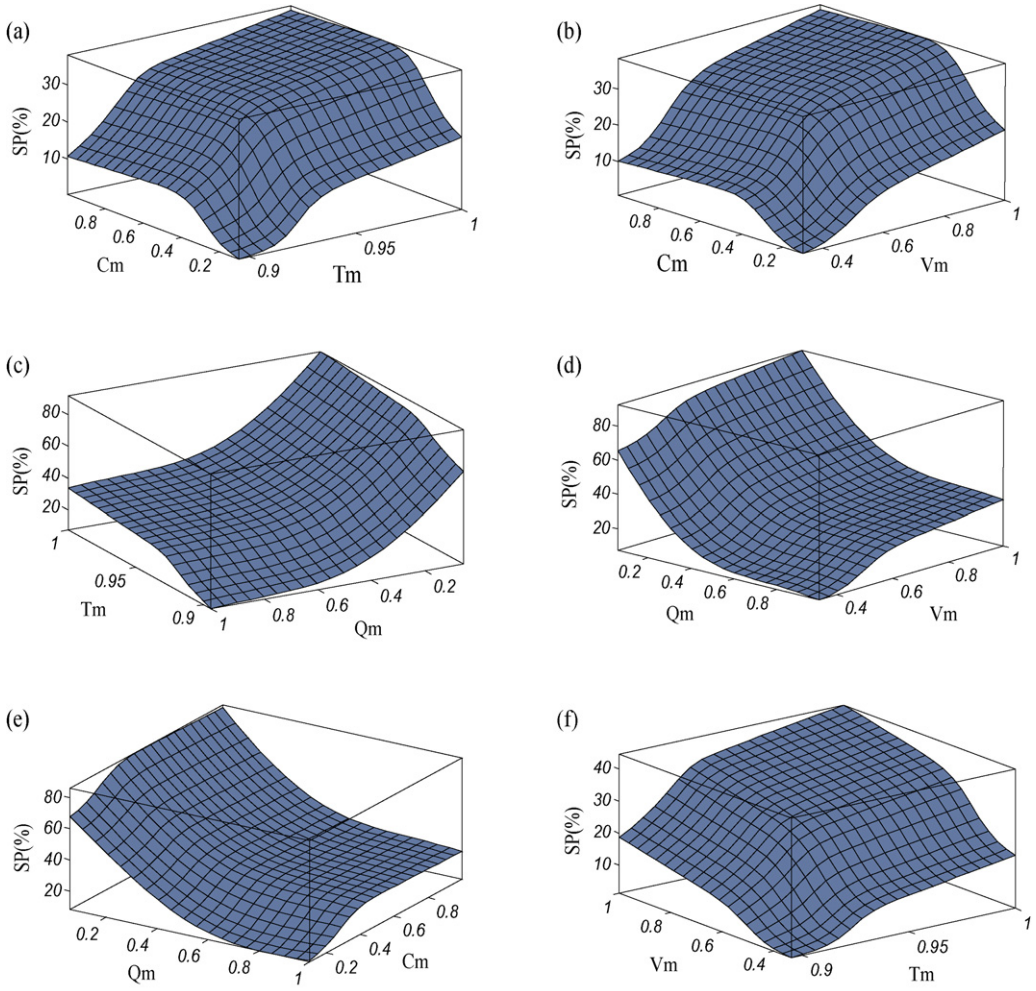

Fig. 11. Generalization performances of FL-based model, effects of (a) concentration and temperature at 0.7 mL/s and 20 V, (b) voltage and concentration at 0.7 mL/s and 40 °C, (c) flow rate and temperature at 500 ppm and 20 V, (d) voltage and flow rate at 500 ppm and 40 °C, (e) flow rate and concentration at 20 V and 40 °C, and (f) voltage and temperature at 500 ppm and 0.7 mL/s on SP.

35 extra experiments were carried out at the central points of each factor, i.e. $T = 35$ and 50 °C, $C = 250$ and 750 ppm, $Q = 0.03$ and 0.9 mL/s and $V = 15$ and 25 V.

Hence, data matrix of the ANFIS model structure includes 116 rows and 5 column [116 × 5]. The first four columns of this matrix are operating conditions and the last one is the ED process response (SP). With the aid of MATLAB programming software 101 data was randomly picked up in each run for training and the rest was used for testing. The procedure was repeated until randomly chosen training data led to MSRE of less than 0.01 for training and testing data.

Standard artificial intelligence tools such as neural network and FL need three subsets of data: training, validating and testing. However, validating subset is used only for noisy systems. In most of control systems where dynamic problems are dealt, validating subset is also applied. In the present work, SP of an ED cell was acquired at steady state condition. Hence, the necessity of utilizing validating data set was not met.

When normal values of input variables (as mentioned above) were used, prediction of SP values lower than 10 was impossible. Therefore, a new set of non-dimensional parameters was defined through dividing each input variable by its highest value (e.g. 10/30, 20/30 and 30/30 for voltage).

The ANFIS model structure applied for training and testing of the model is illustrated in Fig. 9. As can be seen, it includes 4 input variables, 2 Gaussian membership functions for each variable and 16 (2^4) rules. It should be noted that, when two membership functions are considered for four variable, 16 unique rules will be obtained using every tool. In this study, 80 linear parameters and 16 nonlinear parameters were obtained by the ANFIS approach. T_m, C_m, V_m and Q_m in Fig. 9 are non-dimensional parameters.

5.1.3. FL model performance

Different groups of training data were examined and with respect to the mean squared error (MSE) of testing data, the proper model was developed. MSE is calculated as follows:

$$\mathrm{MSE} = \frac{\sum_N (\mathrm{SP_{cal}} - \mathrm{SP_{exp}})^2}{N} \quad (20)$$

where subscripts cal and exp denote calculated and experimental values of SP, respectively. N is the number of testing and training data.

The most widely used criteria including MSE, root mean square error (RMSE), correlation coefficient (R), coefficient of determination (R^2) and MSRE for training and testing data sets are presented in Table 4. RMSE is the square root of MSE presented in Eq. (20). In probability theory and statistics, R indicates the strength and direction of a linear relationship between two variables. In general statistical usage, R refers to the departure of two variables from independence. A number of different coefficients are used for different situations. The best known is the Pearson product-moment

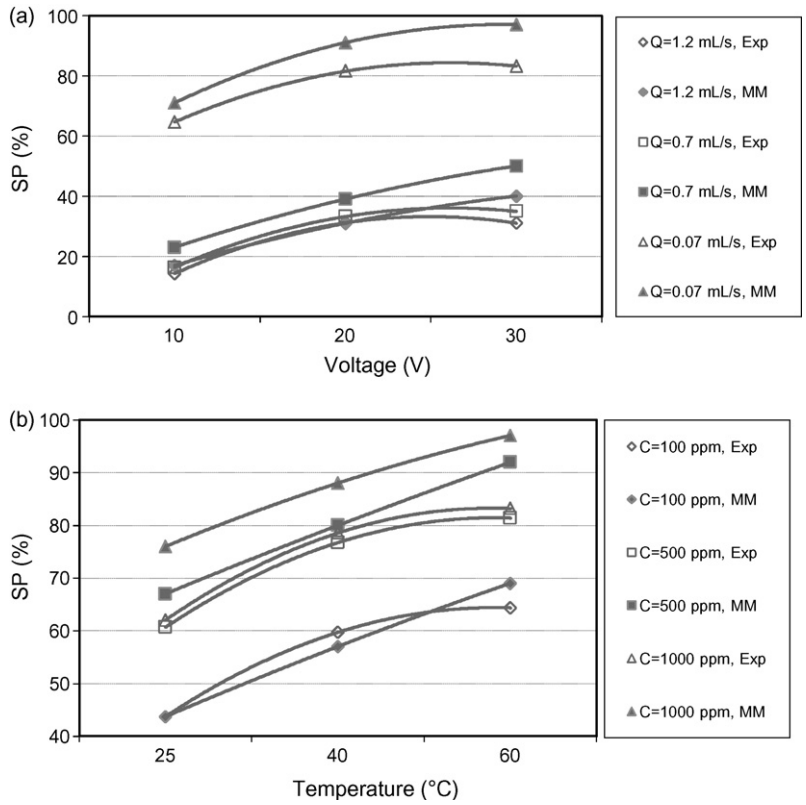

Fig. 12. MM prediction values compared with experimental data, effect of (a) voltage on SP at different flow rates, (b) temperature on SP at different feed concentrations, both plotted at optimum levels of two other factors, i.e. C = 1000 ppm, T = 60 °C, Q = 0.07 mL/s and V = 30 V.

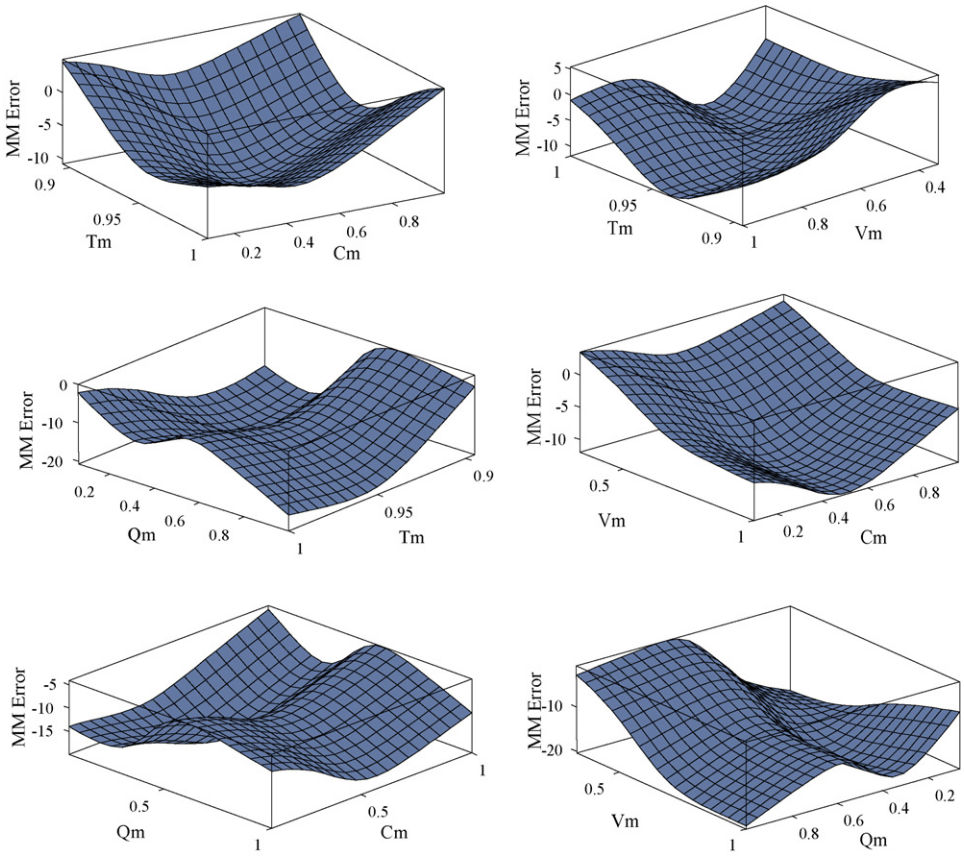

Fig. 13. MM error as a function of operating parameters.

correlation coefficient as follows:

$$R = \frac{\sum_N (SP_{cal} - SP_{cal,ave})(SP_{exp} - SP_{exp,ave})}{\sqrt{\sum_N (SP_{cal} - SP_{cal,ave})} \times \sqrt{\sum_N (SP_{exp} - SP_{exp,ave})}} \quad (21)$$

R^2 can have only positive values ranging from $R^2 = +1.0$ for a perfect correlation (positive or negative) down to $R^2 = 0.0$ for a complete absence of correlation. The advantage of R is that it provides the positive or negative direction of the correlation. The advantage of R^2 is that it provides a measure of the strength of the correlation. It can be said that R^2 represents the proportion of the data that is the closest to the line of best fit.

Another measure of fit is MSRE which is calculated by the following equation:

$$MSRE = \frac{1}{N}\sum_N \left(\frac{SP_{cal} - SP_{exp}}{SP_{exp}}\right)^2 \quad (22)$$

In Fig. 10, the experimental results (training and testing data) versus fuzzy model predictions are plotted. According to this figure and data presented in Table 4, excellent fitness of fuzzy predicted values with experimental data is realized.

5.1.4. Generalization of the FL-based model

After developing an efficient FL-based model, it can be used for prediction of SP for different inputs in the domain of training data. In Fig. 11, predicted values of SP are plotted versus operating parameters in 3D plots. As can be observed, increasing temperature (Fig. 11a,c,f), concentration (Fig. 11a,b,e) and voltage (Fig. 11b,d,f) increases SP values. It is obviously due to the fact that increasing temperature and concentration decreases electrical resistance of the solution, while increasing voltage increases driving force of the process. At higher flow rates, SP values decreases because the more flow rate means the less residence time, and thus, ions that are between the membranes do not have enough time to transfer through them (Fig. 11c,d,e) [5,6,20,53,54].

Taking a closer look to Fig. 11, it is found that the differences between SP values regarding medium and high levels of parameters are negligible comparing to those regarding low and medium levels, i.e., at higher values of parameters, almost constant values of SP are achieved.

When voltage, concentration and temperature increase, concentration polarization phenomenon becomes more important. Intensified concentration polarization adjacent to the ion exchange membranes, reduces SP in an obvious manner. On the other hand, capability of ion exchange membranes with certain surface area is also limited. This capability is characterized by ion exchange capacity (IEC) of the membranes presented in Table 2. It means that the mechanism of ion transport through the membranes may not allow zinc ions to transfer, even if operating condition becomes more favorable. Higher amounts of feed flow rate than 0.7 mL/s have almost no effect on separation performance. It means that, at higher flow rate than 0.7 mL/s, residence time of ions in dilute compartment reaches to its minimum value and consequently electrical potential is not induced on ions. Hence, SP approaches to a constant minimum value at higher flow rates.

The corresponding generalization performances of the developed model, as indicated in Fig. 11, show no oscillations, and this confirms an excellent prediction performance of the FL-based model.

5.2. MM performance

In order to assess the reliability of MM, the calculated results were compared with the measured experimental data. MM prediction values and experimental data are depicted in Fig. 12. As can be seen in Fig. 12a, MM predicts reasonable results at low and medium voltages ($10 < V < 20$ V) and all flow rates with coefficient of determination, R^2, of higher than 0.975.

Table 5
Comparing of the performance of MM and ANN model.

Criterion	MM	FL	MM–FL Coupled Model
MSE	38.605	0.2712	0.7101
RMSE	6.213	0.5208	0.8501
R	0.975	0.9998	0.9991
R^2	0.950	0.9997	0.9982
MSRE	23.949	0.0074	0.0470

According to Fig. 12b, it is found that there is an acceptable agreement ($R^2 > 0.970$) between the calculated results and experimental data at lower temperatures and concentrations ($100 < C < 500$ ppm and $25 < T < 40$ °C). However, the range of one parameter at which MM gives reasonable responses is significantly dependent on adjustments of other parameters. For example, at higher flow rates, MM error is minimized at lower voltages while at lower flow rates this result is inverted. Altogether, when nonlinearity of ED process increases, MM error increases obviously. It seems that at higher values of voltage, concentration and temperature, predicting the behavior of ED process becomes more difficult (Fig. 11). It is due to the intensification of concentration polarization at higher values of theses parameters, as discussed before.

It should be noted that, although experimental values and MM curves do not completely coincide with each other (significant deviations are observed in some cases), they properly describe the trend of the behavior. Obviously, it can be said that MM is of great importance because (1) it satisfies experimental data to a moderately sufficient degree of correlation coefficient (0.97); (2) it can

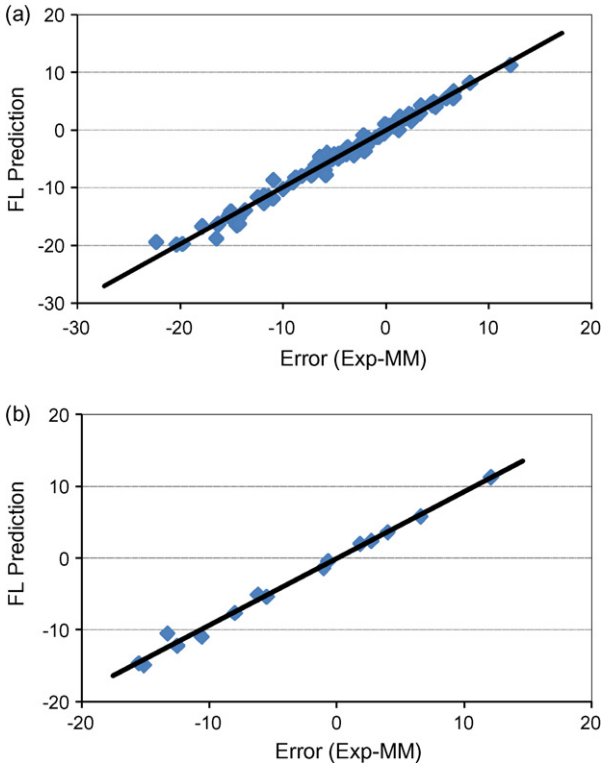

Fig. 14. Performance of FL in predicting the MM error: (a) training data, (b) testing data.

be used for different scale of ED cells and ions; (3) it can be easily used to calculate SP at different operational conditions and (4) it can be used for scale-up. However, coupling MM and FL models, results in more accurate SP values along with other benefits of MM.

5.3. Coupled MM–FL performance

MM error was calculated at all operating conditions. Average absolute error of MM for 81 experiments was evaluated to be 7.5%. 3D plots of MM errors at various operating conditions are shown in Fig. 13. The MM resulted in minimum errors at lower values of feed temperatures, concentrations and cell voltages and medium values of flow rates. As mentioned earlier, at higher values of operating parameters, ED process exhibits more non-linear behavior which consequently increases MM errors. As can be seen in Fig. 13, the MM error was not an intricate function of operating parameters. Hence, the FL model was applied to predict the MM errors. Performance of the FL model in predicting the MM errors is presented in Fig. 14. As observed, there is a superb agreement between the estimated results obtained by the FL model and the experimental data.

The procedure of coupling MM and FL model is well described by a flow chart presented in Fig. 15. At first, SP of zinc ions at various operating conditions and ED cell dimensions is estimated using the MM. Then, the predicted value of MM error by the FL model is added to it to acquire a more accurate response. The FL, MM and coupled MM–FL modeling predictions and the experimental data are juxtaposed in Fig. 16. As can be seen, the FL and coupled MM–FL models can predict SP of the ED cell at various operating conditions much better than the MM. Better performance of the FL and coupled MM–FL models is also confirmed by comparing MSE, RMSE, R, R^2 and MSRE values of the three models in Table 5. As discussed earlier, the MM can be used for different sizes of ED cells and ions which rationalize its application despite much lower accuracy compared with the FL. The developed

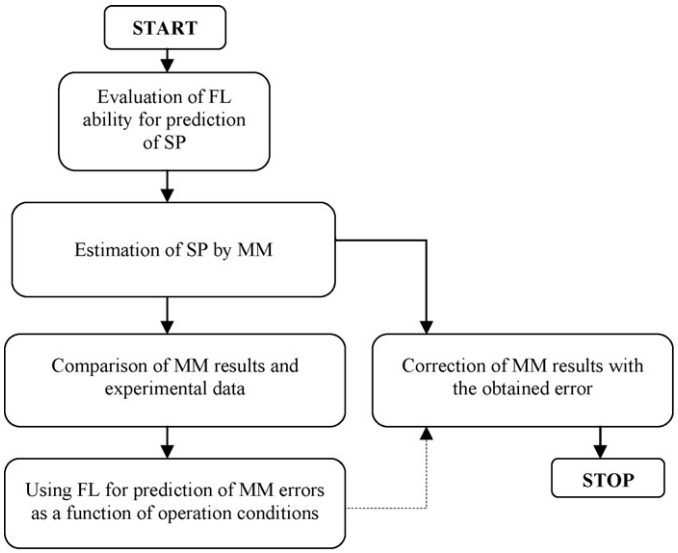

Fig. 15. Flow chart of coupling MM and FL model.

coupled MM–FL model gives SP of zinc ions at various operating conditions as well as different ED cell dimensions with reasonable accuracy.

Excellent agreement between the FL model results and the experimental data indicates the capability of FL to model the complicated ion transfer mechanism in an electrical field. However, the lines of intense curvature in the FL model, which are caused by overtraining, make sensibility of the FL model for interpolation of new patterns uncertain. Fig. 16 confirms that the MM tends to describe the non-linear behavior of the ED process in almost a linear manner. Hence, the lines of mild curvature obtained by the coupled MM–FL model give more reliable results than the FL model and the MM.

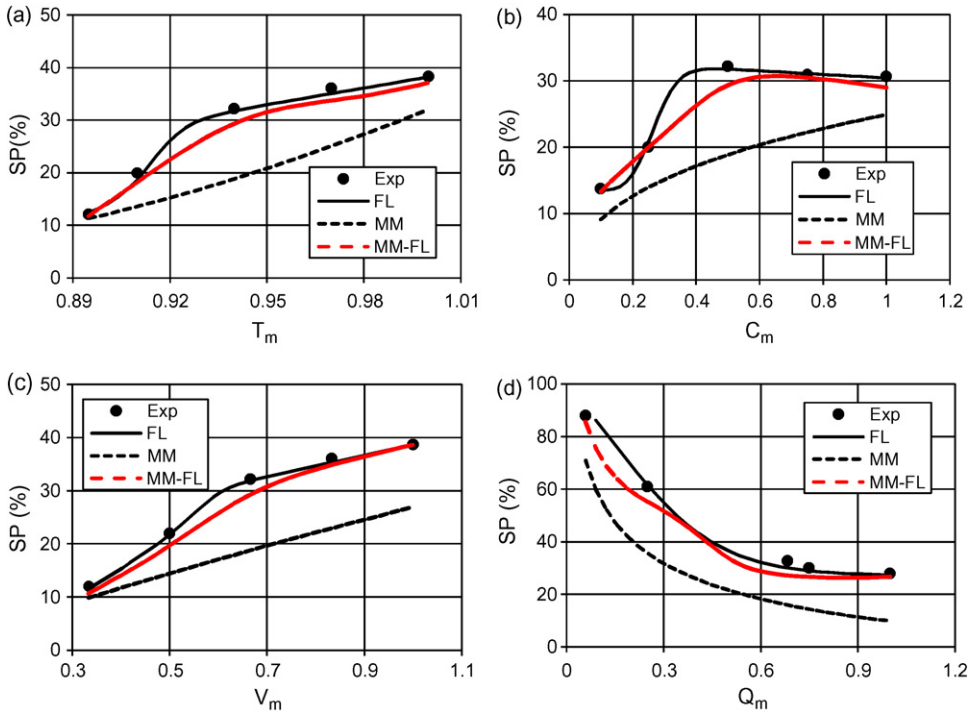

Fig. 16. Comparing MM, FL, MM–FL and experimental data; effect of (a) temperature, (b) concentration, (c) voltage and (d) flow rate on SP at medium levels of other factors, i.e. C = 500 ppm, T = 40 °C, Q = 0.7 mL/s and V = 20 V.

6. Conclusion

In this paper, a Sugeno type fuzzy model was initially developed to predict SP of zinc ions in the dilute compartment of a laboratory scale ED cell. Data spaces were partitioned into fuzzy sets by means of the grid partitioning method. ANFIS methodology was applied to estimate the parameters of the applied two-parametric Gaussian membership function. Then, a previously developed MM was presented. The MM derived from a differential equation of steady state mass balance. Neglecting resistances of ion exchange membranes compared with resistances of bulk solutions in the dilute and the concentrate compartments and deriving a relation for solution resistance as a function of operating parameters, the final one-parameter model was obtained. The MM could be easily used to calculate SP at different operational conditions, ED cell dimensions and ions. However, it could not satisfy the experimental data as well as the FL model. MSE values of FL and MM were 0.27 and 38.60, respectively. Hence, MM and FL were coupled with each other to bring worthwhile privileges of the two models together. The developed coupled model successfully tracked the non-linear behavior of SP versus temperature, voltage, concentration and flow rate with MSE, R and MSRE of 0.710, 0.998 and 0.047, respectively. For almost all the experiments, the developed coupled model (MM–FL) was confirmed to be an adequate interpolation tool for excellent prediction. The MM–FL model integrated many favorable features of theoretical and empirical models such as efficiency, generalization, simplicity and scale-up, and as a result, it can be recommended as an attractive choice for modeling of complex systems, such as wastewater treatment processes.

7. Notation

a	hydrodynamic radius of ion (m)
A	effective area (m^2), fuzzy set
c	centre of the fuzzy set, constant in FL output function
C	concentration ($kmol\,m^{-3}$)
D	diffusivity ($m^2\,s^{-1}$)
e	electronic charge (C)
E	electrical potential (V)
f	function
F	Faraday constant ($C\,kmol^{-1}$)
FL	fuzzy logic
h	thickness of dilute compartment (m)
i	current density ($A\,m^{-2}$)
I	current intensity (A)
J	molar flux ($kmol\,m^{-2}\,s^{-1}$)
k	mass transfer constant ($m\,s^{-1}$)
K	Kohlrausch coefficient ($S\,m^2\,kmol^{-1}\,M^{-0.5}$)
l	flow length in channel (m)
m	a cut of MF
MF	membership function
MM	mathematical model
MSE	mean squared error
MSRE	mean squared relative error
n	number of input variables
N	number of cell pairs, number of testing and training data in FL
P^r	occurrence probability in FL
q	constant
Q	flow rate ($m^3\,s^{-1}$)
r	number of IF–THEN rules
R	resistance (Ω), correlation coefficient, IF–THEN inference rule in FL
$\Re$	universal gas constant ($J\,kmol^{-1}\,K^{-1}$)
R^2	coefficient of determination
RMSE	root mean square error
SP	separation percent (%)
T	temperature (K)
u	flow velocity ($m\,s^{-1}$)
U	n-dimensional Euclidean space in FL
w	width of ED cell (m)
x	coordinate (m)
x'	constant ($C^2\,s\,kmol^{-1}\,kg^{-1}$)
X	input variable in FL
y'	constant ($S\,m^2\,kmol^{-1}\,M^{-0.5}$)
Y	output of FL
z	valence
z'	constant ($M^{-0.5}$)

Greek letters

α	cut in FL
β	constant ($kmol\,K^{2/3}\,s^{1/3}\,m^{-7/3}\,kg^{-2/3}\,A^{-1}$)
γ	constant (s^{-1})
γ'	constant ($s\,m^{-1}$)
δ	constant
ε	electric permittivity ($C^2\,J^{-1}\,m^{-1}$)
ε_0	permittivity in free space ($C^2\,J^{-1}\,m^{-1}$)
ε_r	relative permittivity
ζ	Debye–Huckel–Onsager coefficient ($S\,m^2\,kmol^{-1}\,M^{-0.5}$)
η	current efficiency
θ	constant
κ	conductivity ($S\,m^{-1}$)
λ	molar conductivity of ions ($S\,m^2\,kmol^{-1}$)
Λ_M	molar conductivity ($S\,m^2\,kmol^{-1}$)
Λ_M°	limiting molar conductivity ($S\,m^2\,kmol^{-1}$)
μ	viscosity ($kg\,m^{-1}\,s^{-1}$), symmetric Gaussian function in FL
ν	stoichiometric constant
ρ	density ($kg\,m^{-3}$)
σ	width of the fuzzy set in FL
υ	mobility of ions ($m^2\,s^{-1}\,V^{-1}$)
φ	constant ($m^{4/3}\,s^{2/3}\,kg^{2/3}\,A\,kmol^{-1}\,K^{-2/3}$)
ψ	Debye–Huckel–Onsager coefficient ($M^{-0.5}$)
ω	constant

Subscript

$\pm$	cation or anion
0	initial condition
cal	calculated
d	dilute compartment
exp	experimental
m	membrane
M	molar

References

[1] R.W. Baker, E.L. Cussler, W. Eykamp, W.J. Koros, R.L. Riley, H. Strathmann, Membrane Separation Systems, Noyes Data Corporation, New Jersey, 1991.
[2] W.S. Winston Ho, K.K. Sirkar, Membrane Handbook, Champan & Hall, New York, 1992.
[3] M. Mulder, Basic Principles of Membrane Technology, Kluwer, Dordrecht, 1996.
[4] T. Mohammadi, A. Kaviani, Water shortage and seawater desalination by electrodialysis, Desalination 158 (2003) 267–270.
[5] T. Mohammadi, A. Moheb, M. Sadrzadeh, A. Razmi, Separation of copper ions by electrodialysis using Taguchi experimental design, Desalination 169 (2004) 21–31.
[6] T. Mohammadi, A. Razmi, M. Sadrzadeh, Effect of operating parameters on Pb^{2+} separation from wastewater using electrodialysis, Desalination 167 (2004) 379–385.
[7] W.Y. Lee, G.G. Park, T.H. Yang, Y.G. Yoon, C.S. Kim, Empirical modeling of polymer electrolyte membrane fuel cell performance using artificial neural networks, Int. J. Hydrogen Energ. 29 (2004) 961–966.
[8] A. Shahsavand, M. Pourafshari Chenar, Neural networks modeling of hollow fiber membrane processes, J. Mem. Sci. 297 (2007) 59–73.
[9] G.B. Sahoo, C. Ray, Predicting flux decline in cross-flow membranes using artificial neural networks and genetic algorithms, J. Mem. Sci. 283 (2006) 147–157.

[10] K.S. Spiegler, Polarization at ion exchange membrane–solution interfaces, Desalination 9 (1971) 367–385.
[11] C. Forgacs, N. Ishibashi, J. Leibovitz, J. Sinkovic, K.S. Spiegler, Polarization at ion-exchange membranes in electrodialysis, Desalination 10 (1972) 181–214.
[12] T.C. Huang, I.Y. Yu, S.B. Lin, Ionic mass transfer rate of $CuSO_4$ in electrodialysis, Chem. Eng. Sci. 38 (1983) 1873–1879.
[13] A.T. Cherif, C. Gavach, Electro-transport of sulphuric acid by electro-electrodialysis, J. Electroanal. Chem. 265 (1989) 143–157.
[14] T.C. Huang, J.K. Wang, Preferential transport of nickel and cupric ions through cation exchange membrane in electrodialysis with a complex agent, Desalination 86 (1992) 257–271.
[15] J.A. Wesselingh, P. Vonk, G. Kraaijeveld, Exploring the Maxwell–Stefan description of ion exchange, Chem. Eng. J. Biochem. Eng. J. 57 (1995) 75–89.
[16] G. Kraaijeveld, V. Sumberova, S. Kuindersma, H. Wesselingh, Modeling electrodialysis using the Maxwell–Stefan description, Chem. Eng. J. Biochem. Eng. J. 57 (1995) 163–176.
[17] Y. Tanaka, Concentration polarization in ion-exchange membrane electrodialysis—the events arising in a flowing solution in a desalting cell, J. Mem. Sci. 216 (2003) 149–164.
[18] V. Nikonenko, K. Lebedev, J.A. Manzanares, G. Pourcelly, Modeling the transport of carbonic acid anions through anion-exchange membranes, Electrochim. Acta 48 (2003) 3639–3650.
[19] J. Shen, J. Duan, Y. Liu, Y. Lixin, X. Xing, Demineralization of glutamine fermentation broth by electrodialysis, Desalination 172 (2005) 129–135.
[20] T. Mohammadi, A. Moheb, M. Sadrzadeh, A. Razmi, Modeling of metal ion removal from wastewater by electrodialysis, Sep. Purif. Technol. 41 (2005) 73–82.
[21] M. Fidaleo, M. Moresi, Optimal strategy to model the electrodialytic recovery of a strong electrolyte, J. Mem. Sci. 260 (2005) 90–111.
[22] B. Ruiz, P. Sistat, G. Pourcelly, Patrice Huguet Electromembrane process with pulsed electric field, Desalination 199 (2006) 62–63.
[23] A. Pismenskiy, V. Nikonenko, M. Urtenov, G. Pourcelly, Mathematical modeling of gravitational convection in electrodialysis processes, Desalination 192 (2006) 374–379.
[24] M. Sadrzadeh, A. Kaviani, T. Mohammadi, Mathematical modeling of desalination by electrodialysis, Desalination 206 (2007) 538–546.
[25] S. Koter, Modeling of weak acid production by the EDB method, Sep. Purif. Technol. 57 (2007) 406–412.
[26] S. Koter, Separation of weak and strong acids by electro-electrodialysis: experiment and theory, Sep. Purif. Technol. 60 (2008) 251–258.
[27] M.P. Mier, R. Ibanez, I. Ortiz, Influence of ion concentration on the kinetics of electrodialysis with bipolar membranes, Sep. Purif. Technol. 59 (2008) 197–205.
[28] J.A. Moleon, A.A. Moya, Network simulation of the electrical response of ion-exchange membranes with fixed charge varying linearly with position, J. Electroanal. Chem. 613 (2008) 23–34.
[29] R. Krishna, J.A. Wesselingh, The Maxwell–Stefan approach to mass transfer, Chem. Eng. Sci. 52 (1997) 861–911.
[30] J.H.G. van der Stegen, A.J. van der Veen, H. Weerdenburg, J.A. Hogendoorn, G.F. Versteeg, Application of the Maxwell–Stefan theory to the transport in ion-selective membranes used in the chloralkali electrolysis process, Chem. Eng. Sci. 54 (1999) 2501–2511.
[31] M. Sadrzadeh, T. Mohammadi, J. Ivakpour, N. Kasiri, Separation of lead ions from wastewater using electrodialysis: comparing mathematical and neural network modeling, Chem. Eng. J. 144 (2008) 431–441.
[32] E.I. Tiffee, A. Weber, K. Schmid, V. Krebs, Macroscale modeling of cathode formation in SOFC, Solid State Ionics 174 (2004) 223–232.
[33] J.O. Schumacher, P. Gemmar, M. Denneb, M. Zedda, M. Stueber, Control of miniature proton exchange membrane fuel cells based on fuzzy logic, J. Power Source 129 (2004) 143–151.
[34] A. Zilouchian, M. Jafar, Automation and process control of reverse osmosis plants using soft computing methodologies, Desalination 135 (2001) 51–59.
[35] D. Hissel, M.C. Pera, J.M. Kauffmann, Diagnosis of automotive fuel cell power generators, J. Power Source 128 (2004) 239–246.
[36] M. Tekin, D. Hissel, M.C. Pera, J.M. Kauffmann, Energy consumption reduction of a PEM fuel cell motor–compressor group thanks to efficient control laws, J. Power Source 156 (2006) 57–63.
[37] H.B. Shen, J. Yang, K.C. Chou, Fuzzy KNN for predicting membrane protein types from pseudo-amino acid composition, J. Theor. Biol. 240 (2006) 9–13.
[38] K.V. Kilimann, C. Hartmann, A. Delgado, R.F. Vogel, M.G. Ganzle, A fuzzy logic-based model for the multistage high-pressure inactivation of *Lactococcus lactis* ssp. cremoris MG 1363, Int. J. Food Microbiol. 98 (2005) 89–105.
[39] M.G. Ganzle, K.V. Kilimann, C. Hartmann, R. Vogel, A. Delgado, Data mining and fuzzy modeling of high pressure inactivation pathways of *Lactococcus lactis*, Innovat. Food Sci. Emerg. Technol. 8 (2007) 461–468.
[40] H. Takagi, I. Hayashi, NN-driven fuzzy reasoning, Int. J. Approx. Reason. 5 (1991) 191–212.
[41] J.T. Ross, Fuzzy Logic with Engineering Applications, McGraw Hill, Inc., New York, USA, 1995.
[42] C.L. Karr, E.J. Gentry, Fuzzy control of pH using genetic algorithms, IEEE Trans. Fuzzy Syst. 1 (1993) 46–53.
[43] Y. Yoshinari, W. Pedrycz, K. Hirota, Construction of fuzzy models through clustering techniques, Fuzzy Set Syst. 54 (1993) 157–165.
[44] D. Dubois, H. Prade, Fuzzy Sets and Systems: Theory and Applications, Academic, New York, USA, 1980.
[45] T. Takagi, M. Sugeno, Fuzzy identification of systems and its application to modeling and control, IEEE Trans. Syst. Man Cybern. 15 (1985) 116–132.
[46] J.S.R. Jang, ANFIS: adaptive network based fuzzy inference system, IEEE Trans. Syst. Man Cybern. 23 (1993) 665–684.
[47] M. Demircioglu, N. Kabay, Cost comparison and efficiency modeling in the electrodialysis of brine, Desalination 136 (2001) 317–323.
[48] A.A. Sonin, M.S. Isaacson, Optimization of flow design in forced flow electrochemical systems, with special application to electrodialysis, Ind. Eng. Chem. Proc. Des. Dev. 13 (1974) 241–248.
[49] N. Kabay, M. Ardab, L. Kurucaoval, P.E. Ersoza, H. Kahveci, M. Can, S. Dal, Effect of feed characteristics on the separation performances of monovalent and divalent salts by electrodialysis, Desalination 158 (2003) 95–100.
[50] M.C. Porter, Handbook of Industrial Membrane Technology, Noyes Publications, New Jersey, 1990.
[51] R.W. Rousseau, Handbook of Separation Process Technology, John Wiley and Sons, Inc., New York, 1987.
[52] R. Klischenko, B. Kornilovich, R. Chebotaryova, V. Linkov, Purification of galvanic sewage from metals by electrodialysis, Desalination 126 (1999) 159–162.
[53] M. Sadrzadeh, A. Razmi, T. Mohammadi, Separation of different ions from wastewater at various operating conditions using electrodialysis, Sep. Purif. Technol. 54 (2007) 147–156.
[54] M. Sadrzadeh, A. Razmi, T. Mohammadi, Separation of monovalent, divalent and trivalent ions from wastewater at various operating conditions using electrodialysis, Desalination 205 (2007) 53–61.